The 2018-2019 weak El Niño: predicting the risk of a dengue outbreak in Machala, Ecuador

Desislava Petrova*[1], Xavier Rodó[1,2], Rachel Sippy[3], Joan Ballester[1], Raul Mejía[4], Efraín Beltrán-Ayala[5], Mercy J. Borbor-Cordova[6], G. Mauricio Vallejo[7], Alberto A. Olmedo[7], Anna M. Stewart-Ibarra[3], Rachel Lowe[1,8,9]

November 24, 2020

1. Climate and Health Programme, Barcelona Institute for Global Health (ISGlobal), Doctor Aiguader 88, 1a planta, tel. +34 93 7331, Barcelona, Catalonia, Spain

2. Institució Catalana de Recerca i Estudis Avancats (ICREA), Barcelona, Catalonia, Spain

3. Institute for Global Health and Translational Science, SUNY Upstate Medical University, Syracuse, NY, USA

4. Instituto Nacional de Meteorología e Hidrología, Guayaquil, Guayas Province, Ecuador

5. Facultad de Medicina, Universidad Tecnica de Machala, Machala, El Oro Province, Ecuador

6. Facultad de Ingeniería Maritima y Ciencias del Mar, Escuela Superior Politecnica del Litoral, ESPOL, Guayaquil, Ecuador

7. Ministry of Health of Ecuador, Department of Epidemiological Surveillance, Quito, Ecuador

8. Centre for Mathematical Modelling of Infectious Diseases, London School of Hygiene and Tropical Medicine, London, UK

9. Centre on Climate Change and Planetary Health, London School of Hygiene and Tropical Medicine, London, UK

***Corresponding author email: desislava.petrova@isglobal.org**

Abstract

Sea surface temperature conditions in the central-eastern tropical Pacific have indicated a mild El Niño event since October 2018, which currently continues throughout the spring of 2019. The global El Niño Southern Oscillation (ENSO) forecast consensus is that these generally weak warm patterns will persist at least until the end of the summer. El Niño and its impact on local climatic conditions in southern coastal Ecuador influences the inter-annual transmission of dengue fever in the region. In this study we use an ENSO model to issue forecasts of El Niño for the year 2019, which are then used to predict local climate variables, precipitation and minimum temperature, in the city of Machala, Ecuador. All these forecasts are incorporated in a dengue transmission model, specifically developed and tested for this area, to produce out-of-sample predictions of dengue risk. Predictions are issued at the beginning of January 2019 for the whole year, thus providing the longest forecast lead time of 12 months. Preliminary results indicate that the mild and ongoing El Niño event did not provide the optimum climate conditions for dengue transmission, with the model predicting a very low probability of a dengue outbreak during the typical peak season in Machala in 2019. This is contrary to 2016, when a large El Niño event resulted in excess rainfall and warmer temperatures in the region, and a dengue outbreak occurred 3 months earlier than expected. This event was successfully predicted using a similar prediction framework to the one applied here. With the present study we continue our efforts to build and test a climate service tool to issue early warnings of dengue outbreaks in the region.

1 Introduction

Climate is a major driver of dengue incidence and epidemics globally. Regional patterns of climate, which are influenced by the El Niño Southern Oscillation (ENSO) phenomenon, have been linked to recurring outbreaks of dengue in many locations (Anyamba et al., 2019; Huang et al., 2015; Lowe et al., 2017; Sippy et al., 2019; Vincenti-Gonzalez et al., 2018; Xiao et al., 2018). These studies have also used measures of local climate conditions, such as temperature, humidity and precipitation, to understand variations in dengue incidence (Huang et al., 2015; Sippy et al., 2019; Duarte et al., 2019; Zhang et al., 2019). In a series of previous studies (Stewart-Ibarra and Lowe, 2013; Lowe et al., 2017; Petrova et al., 2019) we demonstrated that climate information and in particular local seasonal climate and ENSO forecasts can be used to improve the prediction of dengue outbreaks in southern coastal Ecuador in El Oro Province, and more importantly, to extend the lead time of such predictions to several seasons in advance. Both temperature and rainfall are known to affect the physiology of the dengue vectors *Aedes aegypti* and *Aedes albopictus mosquitoes* in terms of their larval development and replication rates (Mordecai et al., 2017). The optimal temperature for dengue transmission has been found to be between 26-29°C (Mordecai et al., 2017). The abundance or scarcity of rainfall can increase larval mosquito habitats depending on local access to piped water and local storage practices (Stewart Ibarra, Ryan and Beltran, 2013; Lowe et al., 2018). ENSO is known to affect climate patterns through atmospheric teleconnections (Ropelewski and Halpert, 1987; Kiladis and Diaz, 1989; Rodó, Rodriguez-Arias and Ballester, 2006; Sarachik and Cane, 2010), and southern coastal Ecuador is typically associated with heavy rainfall during and after El Niño events (Larkin and Harrison, 2002; Rossel and Cadier, 2009; Petrova et al., 2019). Moreover, due to the proximity of El Oro Province to the equatorial Pacific area where ENSO occurs, its impact on local temperature is also well-understood with increased temperature during and after the warm events (Aceituno, 1988; Bendix and Bendix, 2006; Santos, 2006; Rossel and Cadier, 2009; Moran-Tejeda et al., 2016). Generally, the climatological precipitation and temperature rates are enhanced during El Niño years (Petrova et al. (2019); Figure 1).

Dengue is hyperendemic in coastal Ecuador and presents a high burden of disease, particularly in young people under 20 years of age (Stewart Ibarra et al., 2018). A dengue early warning system would allow the public health sector to better prevent and respond to dengue outbreaks, for example, through community mobilization, training of physicians, procurement of diagnostics and insecticides, and elimination of vector habitat (Stewart Ibarra et al., 2019). Every year the same number of cases is expected as in previous years, as well as a peak in transmission during the warm and wet season (Stewart-Ibarra and Lowe, 2013), which is typically between January and May (Moran-Tejeda et al., 2016). Current epidemic surveillance practices consist of monitoring the seasonal evolution of dengue compared to the monthly mean incidence calculated using retrospective dengue case reports from the past 5 years (Lowe et al., 2017). Importantly, local climate and ENSO information is not included in these calculations. In order to improve the dengue forecast, in the last several years we designed and tested a prediction framework for dengue in El Oro Province and in its capital city of Machala, in which local minimum temperature, precipitation, and ENSO forecasts are used within a Bayesian hierarchical dengue model, to predict dengue outbreaks a few seasons in advance (Stewart-Ibarra and Lowe, 2013; Lowe et al., 2017; Petrova et al., 2019). These studies found that ENSO was the most important climatic predictor in the dengue model. In 2016, when one of the strongest El Niño events on record occurred (CPC, 2017), we tested the prediction framework in real time and managed to successfully issue probabilistic forecasts of dengue incidence in the city of Machala, from January to November 2016 (Lowe et al., 2017).

In the present study, we similarly document a real-time forecast of the dengue season in 2019, following the weak, indeed borderline El Niño event that developed at the end of 2018 and beginning of 2019. We define an El Niño event to occur when there are five consecutive 3-month periods with temperature in the Niño3.4 region that exceeds 0.5°C. The aim of this study is to test the prediction system during a mild El Niño year in order to investigate the sensitivity of the system to the amplitude of the warm events, given the importance of ENSO in the dengue model.

El Niño conditions have prevailed in the tropical Pacific since October 2018. As of June 2019, El Niño is still ongoing, with sea surface temperatures (SST) above average, especially in the eastern part of the basin. The wind patterns are also consistent with an El Niño event, with westerly wind anomalies in the western and central equatorial Pacific from January to May 2019 that propagated all the way to the eastern Pacific at the end of May (see the CPC ENSO diagnostic discussion for June). The main area of convection and precipitation has also shifted eastwards towards the central equatorial Pacific since January (CPC, 2019). The warm event is most likely to extend until the end of the summer (70% chance according to the CPC ENSO diagnostic discussion for June) and some models foresee the event lingering until the end of the year. SST anomalies over May-June have been $\sim 1°C$ in the central equatorial Pacific, $\sim 0.7°C$ in the eastern Pacific, and $\sim 1°C$ near the coastal regions of southern Ecuador. The upper-ocean heat content (0-300m depth) has also been above average since early 2018 with a peak in October, while the thermocline has been anomalously deep in the eastern equatorial Pacific. Subsurface temperature anomalies across the whole equatorial Pacific have been positive with slight weakening over the past month, but they increased in the central part of the basin. All of these characteristics are consistent with a mild El Niño event.

In the following sections, we describe the data and methods used to formulate the models, present the forecasts generated by the modelling framework, and discuss the implications of our findings for local decision making.

2 Methods

2.1 Study area

Machala is the capital of El Oro Province, located in southern coastal Ecuador (projected 2019 population: 286,120, location: 3°15' S, 79°57' W, elevation: 9 meters). It features a tropical climate with a rainy (January-May) and dry (July-November) season (Figure 1b) with temperatures ranging from 20.8 to 31.0° Celsius. The city and surrounding area are dominated by agricultural (banana, coffee, and cacao), aquacultural (shrimp), and mining industries; Machala is also a commercial shipping hub due to its proximity to Peru, the presence of a major port, and transportation routes (via the Pan-American highway or the Pacific coast).

Machala has high burden of dengue, chikungunya, and Zika with strong seasonal patterns of arbovirus transmission (Stewart-Ibarra et al., 2017). Depending on the year, all four dengue serotypes (DENV 1-4) may be in co-circulation (Stewart Ibarra et al., 2018). Healthcare services for the diagnosis of arboviral infections are readily available, with Ministry of Health clinics providing primary care and a large public health hospital (Hospital Teófilo Dávila, the reference hospital for the province) with more comprehensive healthcare in central Machala.

2.2 Data

2.2.1 Climate data

Predictors in the ENSO model used for the prediction of SST in the Niño3.4 region [120°-170°W, 5°S-5°N] include zonal wind stress, surface and subsurface temperature in different parts of the equatorial Pacific Ocean. Zonal wind stress is obtained from the NCEP/NCAR reanalysis (Kalnay et al., 1996), SST from NOAA-OI-SST-V2 (available at www.esrl.noaa.gov/psd/), and subsurface temperature until 2012 is from the Subsurface Temperature And Salinity Analyses by Ishii et al. (2005), archived at the National Center for Atmospheric Research, Computational and Information Systems Laboratory (www.rda.ucar.edu/datasets/ds285.3/), and from the Hadley Centre EN4.0.2 analyses data (Good, Martin and Rayner, 2013) afterwards.

Local daily weather data, minimum temperature and precipitation in the city of Machala is derived from the Granja Santa Ines weather station (location: 3°17'26" S, 79°54'5" W, elevation: 10 m) and from the Hospital Teófilo Dávila weather station (location: 3°15'35.2" S, 79°57'12.9" W, elevation: 8 m), both located in Machala and operated by the National Institute of Meteorology and Hydrology (INAMHI) of Ecuador.

Monthly summary data (minimum, mean, maximum temperature and total precipitation) were calculated for each weather station. For modelling, summaries from Granja Santa Ines were used from January 2002 to December 2016, and summaries from Hospital Teófilo Dávila were used from January 2017 to present.

2.2.2 Disease surveillance data

Data on the total monthly cases of dengue in Machala were provided by the Ministry of Health of Ecuador for the period January 2002 to present. Cases were diagnosed by clinical presentation, epidemiological nexus, and laboratory diagnostics in some cases. Due to limited resources, only a subset of cases were confirmed by laboratory diagnostics (by ELISA) at the national reference laboratory (INSPI) in Guayaquil.

2.2.3 Population data

Annual population projections were obtained from the Ecuador National Statistics and Census Institute (INEC). These projections are based on the 2010 National Census (Censosnd., 2017).

2.3 ENSO forecast model

The ENSO model used here to predict SST in the Niño3.4 region in 2019 is the dynamics components model described in Petrova et al. (2017, 2020), as well as applied in our previous studies on dengue prediction in El Oro and Machala (Lowe et al., 2017; Petrova et al., 2019). The model is composed of unobserved components - trend, time-varying seasonal cycles, and four cycle components corresponding to inter-annual and decadal variability of SST in the Niño3.4 region, as well as of sets of predictor variables - SST, subsurface temperature and zonal wind stress from different regions in the tropical Pacific Ocean, which are also used at different lead times. The model has been successful in predicting retrospectively the ENSO events in the period 1970-2013 at a lead time of more than 1.5 years, and it predicted operationally the events thereafter with the exception of the 2017/18 La Niña event when the model predicted neutral conditions instead (Petrova et al., 2017, 2020). Forecasts of the Niño3.4 index in 2019 were run using the observed data up until December 2018. In this way, the forecast for January 2019 is a one-month lead forecast, while the forecast for December 2019 is a 12-month lead forecast.

2.4 Local climate forecasting

Monthly minimum temperature (Tmin) and precipitation (precip) in Machala for 2019 were predicted using two unobserved components statistical models (Harvey and Koopman, 2000; Durbin and Koopman, 2012). The two models have the same core structure, but different regression predictor variables are incorporated. The core structure is as follows:

$$\mathrm{y}_t = \mu_t + \psi_t + x_t'\delta + \varepsilon_t$$

where y_t is the dependent variable (Tmin or precip), μ_t is a trend, ψ_t is a time-varying seasonal cyclic component, x_t' represents a regression predictor variable with coefficient δ, and ε_t is a noise term. Minimum temperature from January to December 2019 was forecast using the Niño3.4 SST forecasts from the ENSO model as regression predictors at 1 month lag time. We previously identified the highest correlation of 0.63 between these two variables at lag 1 (Petrova et al., 2019). Precipitation from January to December 2019 was then forecast using the Tmin forecasts obtained in this way as regression predictors at 1 month lag time. We similarly identified the highest correlation between the Tmin and precip variables of 0.42 at lag 1 (Petrova et al., 2019). As for the ENSO model, the trend and seasonal cyclic components are modeled as linear dynamic stochastic functions of time (Harvey and Koopman, 2000). More information about the components is given in (Durbin and Koopman, 2012). This type of models can be put in a state-space framework, in which all unknown parameters associated with the model components (e.g. initial trend, frequency and persistence of the cycle, variances, and the regression variable coefficients) are collected in state and disturbance vectors and estimated simultaneously in a dynamic way using the Kalman Filter (Kalman, 1960). The software packages STAMP, SsfPack and OxMetrics (Koopman, Shephard and Doornik, 2008; Koopman et al., 2010; Doornik, 2013) were used for the estimations of parameters and for forecasting.

2.5 Dengue forecast model

Following Lowe et al. (2017), a Bayesian hierarchical mixed model was fitted to counts of dengue cases from January 2002 to December 2018 using climate data and random effects, and used to produce probabilistic forecasts of dengue cases per month in 2019 (Stewart-Ibarra and Lowe, 2013; Lowe et al., 2013).

$$\begin{gathered}
\mathrm{y}_t \sim NegBin(\mu_t, k) \\
\log(\mu_t) = log(P_{T'(t)}) + \alpha + \beta_{t'(t)} + \gamma_{T'(t)} + \sum \delta_j x_{jt}
\end{gathered}$$

Briefly, dengue cases, y_t, were assumed to follow a negative binomial distribution with mean μ_t and overdispersion parameter k. The model comprises a model offset (log population $P_{T'(t)}$), a random effect to account for seasonality $\beta_{t'(t)}$, $t'(t) = 1, ..., 12$, using a first order autoregressive model, and exchangeable non-structured random effects for each year $\gamma_{T'(t)}$, $T'(t) = 1, ..., 17$, to account for interannual changes in dengue risk attributable to unknown factors between 2002 - 2018, such as changes in vector control practices or the circulation of new serotypes and viruses (e.g. introduction of chikungunya in 2015 and Zika in 2016). The explanatory variables, x_{jt}, included precipitation (x_{1t}) and minimum temperature (x_{2t}), lagged by one month with respect to dengue, and the Niño3.4 index (x_{3t}), lagged by three months with respect to dengue (i.e. two months with respect to the local climate). The model was trained using monthly dengue data from January 2002 - December 2018 and observed climate variables (precipitation, minimum temperature and Niño3.4 index). The model was then used to produce forecasts for January to December 2019, using the Niño3.4 index forecasts and associated precipitation and minimum temperature forecasts (see methods above). Model parameters were estimated in a Bayesian framework using Integrated Nested Laplace Approximation (INLA, www.r-inla.org), and posterior predictive distributions were generated by sampling from an approximated posterior of a fitted model (Lowe et al., 2017).

3 Results

3.1 ENSO forecasts for 2019

Figure 2 shows predictions of SST anomalies in the Niño3.4 region from January to December 2019 at lead times between 1 and 12 months, together with the available observed anomalies until May 2019. The ENSO forecast indicates a slight decrease of SST from February to April 2019 and an increase after May, with a peak anomaly of $\sim 1.4°$C at the end of the year and beginning of 2020 (Figure 2). The forecast underestimates the anomaly between February and April 2019 when compared to the observations. The prediction, however, is consistent with the typical seasonal decay of an El Niño event in spring time. The forecast clearly indicates the return to a warm event after May, and predicts a slightly stronger event for the end of 2019 and the beginning of 2020 than the one at the end of 2018. Note that the mild El Niño event in 2018 was also predicted by the model at 12 months lead time (Figure S1).

3.2 Local climate forecasts for 2019

The minimum temperature forecasts for the city of Machala for 2019 together with the 70% confidence intervals, and the available observed Tmin values from the Hospital Teófilo Dávila weather station until April 2019 are shown in Figure 3. The minimum temperature forecast is also underestimated during the months between February and April 2019. The model for Tmin includes the predicted SST in the Niño3.4 region as a predictor at 1 month lag, as well as a trend, some seasonal effects and noise. It appears that the model in this configuration cannot capture the full variability of the Tmin time series, and some of the warming trend in 2019 is unaccounted for at least until April 2019. Still, the model predicts temperature in 2019 that well exceeds the long-term mean value of Tmin ($\sim 22°$C). The observed temperature in Machala has also been higher than normal since 2015 (Figure 1c), most probably due to the very strong El Niño event that occurred at the end of that year, as well as due to the coastal El Niño event that happened in 2017. The trend in the time series has also increased after 2015, possibly indicating a shift due to the effect of the global climate warming, but it could also be due to the new location of the weather station used for data collection after 2016.

The precipitation forecasts for the city of Machala for 2019 together with the 70% confidence intervals, and the available observed precipitation values from the Hospital Teófilo Dávila weather station until April 2019 are shown in Figure 4. The precipitation forecasts are also underestimated during the months between January and March 2019, but they fall within the 70% CI, and overestimated for the month of April 2019. The model for precipitation includes the minimum temperature forecast as a predictor at 1 month lag, as well as trend, some seasonal effects and noise. It appears that the model cannot capture the full variability in the precipitation time series. The precipitation response in Machala has been variable after mild El Niño events (for e.g. in year 2003 and 2015; Figure 1b) with an increase of the normal precipitation rate after some weak events and a decrease in precipitation after other weak events.

3.3 Probabilistic dengue forecasts for 2019

The model was trained using dengue cases and observed climate data from January 2002 to December 2018. The probabilistic forecasts of dengue incidence for January - December 2019 was then produced using the 2019 climate forecasts as predictors in the dengue model (Figure S2). Figure 5 shows the posterior predicted mean and 95% prediction interval for log dengue incidence rates (cases per 100,000 population) for January to December 2019. The five-year mean dengue incidence (lower threshold; blue curve) and upper 95% confidence interval (upper threshold; red curve), calculated for the period 2014-2018, are included to illustrate the typical thresholds used by the national dengue surveillance system to track dengue outbreaks. In Figure 6, the posterior predictive distribution for each month is shown, indicating the posterior predictive mean (dashed pink curve) and the moving threshold of the upper 95% confidence interval (solid red curve), calculated using incidence over the preceding five years (2014-2018). The probability of exceeding the upper threshold is shown for each month.

The predicted mean was greater than the moving upper threshold in January and February but lower than both thresholds for the majority of the season. The probability of exceeding the upper threshold was 35% in March 2019 (compared to 85% in March 2016, see Lowe et al. (2017)) and 2% in June, the month in which dengue would be expected to peak based on the previous 5 years (Figure 6). The observed dengue incidence data available for 2019 is included (black curve), confirming no dengue outbreaks thus far. The model has successfully distinguished this year as having a lower probability of a dengue outbreak and did not indicate high risk of an early season peak, in contrast to the forecast in 2016 (see Figure S3).

4 Discussion

In this study we used an already tested dynamic components ENSO prediction model (see Petrova et al. (2017); Lowe et al. (2017); Petrova et al. (2020)) to forecast the SST in the Niño3.4 region in 2019. The forecast indicated a continuation of the mild El Niño event from 2018 over the summer, autumn and winter months of 2019, with a slight increase in the warm anomaly at the end of 2019 as compared to the end of 2018. This is in agreement with the International Research Institute (IRI) ENSO forecast (IRI, 2019), which in January 2019 issued a forecast of a mild El Niño event, reaching an amplitude $\sim +0.7°C$ in September-October-November of 2019. Long-lead El Niño forecasts of one or more years ahead of the peak are important mainly due to their implication for more accurate seasonal forecasts in many regions of the world (Sarachik and Cane, 2010). In this case, based on the well-established atmospheric teleconnection between ENSO and the local climate in Ecuador, we used the ENSO forecasts for 2019 with a maximum lead time of 12 months to predict minimum temperature and precipitation in the city of Machala for 2019. This real-time climate forecast information (the ENSO and local climate forecasts) was then incorporated in a dengue prediction framework developed for El Oro Province and the city of Machala, which allowed a prediction of dengue incidence to be made at the start of the year and for the entire dengue season in 2019, something that was only possible through the incorporation of the climate forecasts. The dengue model predicted the dengue incidence to be lower than the mean incidence over the previous 5 years (2014-2018) for the majority of the season, with incidence starting to decline from June onwards as expected by the seasonal evolution of dengue in the region (Figure 5). This decision-support tool can assist public health decision makers in improving the allocation of resources to more pressing issues in 2019, including the migrant crisis from Venezuela, which is currently overwhelming the public health service in Ecuador.

Given the effects of climate on arboviral disease transmission, the World Health Organization and other health experts recommend developing climate services - tools to predict and prevent disease outbreaks (Chen, Chadee and Rawlins, 2006; Trotman et al., 2018), especially in light of the warming climate. These tailored products could include early warning systems or epidemic forecasts. Climate services can provide important timely information to health sector decision makers within the context of a future climate event (Racloz et al., 2012), as we have shown here. The results presented in this study represent a major step forward in the design of a routine operational early warning system for dengue in urban Machala, and demonstrate the ability of the prediction framework to distinguish dengue risk levels during strong (Lowe et al., 2017), but also weak to moderate El Niño years. Future challenges include refining the presentation of probabilistic information and design of the forecasting scheme in consultation with local stakeholders; testing of the model at a larger scale, i.e. for all coastal cities in Ecuador; attracting senior leadership from the climate and health sectors to come together and identify climate services for health as a high priority (ideally with designated resources); agreeing upon a data sharing platform and data-sharing protocols; and increasing the capacity of the health and climate sectors through joint training. Dengue will persist in the region because of the dynamics of the four different dengue serotypes, and other arboviruses (chikungunya, Zika) may also sweep through in periodic outbreaks. Previous experience in Barbados indicates that a dengue model could have a harder time predicting dengue transmission after the introduction of chikungunya and Zika (Lowe et al., 2018). Thus, in the future it is necessary to also test how sensitive the model is to the circulation of these other arboviruses. Another area for improvement of the proposed system is to incorporate information about the spatial diversity of ENSO. There are the so-called Eastern Pacific and Central Pacific El Niño events that project differently on the local climate in southern coastal Ecuador.

Finally, there is an opportunity to include climate services for health and epidemic early warning systems as part of the integrated actions for the implementation of a National Adaptation Plan for the health sector in Ecuador (NDC, 2019). Thus, the early warning system prototype presented here is timely and very relevant for the climate and health communities in the country.

Supporting information

Figure S1: Forecast of the sea surface temperature anomaly (°C) in the Niño3.4 region from January to December 2018 at 12 months lead time (magenta curve), and observation values from January to December 2018 from NOAA-OI-SST-V2. The anomalies are calculated by subtracting the mean annual cycle over the period 1982-2012.

Figure S2: Posterior predicted median (dashed purple curve) and 95% prediction (credible) interval (purple shaded area) for dengue incidence rates (cases per 100,000 population) in Machala, Ecuador, 2002-2018. Observed values for 2002-2018 (solid black curve) and 2019 (data available at time of submission; dashed black curve) are included.

Figure S3: Posterior predicted median (dashed purple curve) and 95% prediction (credible) interval (purple shaded area) for log dengue incidence rates (cases per 100,000 population) in Machala, Ecuador, January - November 2016. The five-year mean dengue incidence (blue curve) and upper 95% confidence interval (red curve), for the period 2011-2015, is shown. Observed dengue incidence rates are also included (dashed black curve).

References

Aceituno, P., 1988. On the functioning of the Southern Oscillation in the South America sector Part I: Sufrace climate. *Monthly Weather Review*, 116, pp.505–524.

Anyamba, A., Chretien, J.P., Britch, S.C., Soebiyanto, R.P., Small, J.L., Jepsen, R., Forshey, B.M., Sanchez, J.L., Smith, R.D., Harris, R. et al., 2019. Global disease outbreaks associated with the 2015–2016 El Niño event. *Scientific reports*, 9, p.1930.

Bendix, A. and Bendix, J., 2006. Heavy rainfall episodes in Ecuador during El Niño events and associated regional atmospheric circulation and SST patterns. *Advances in Geosciences*, 6, pp.43–49.

Censosnd., 2017. Censos, Instituto Nacional de Estadística y N.d. Proyecciones Poblacionales. Instituto Nacional de Estadística y Censos. *http://www.ecuadorencifras.gob.ec/proyecciones-poblacionales/*.

Chen, A.A., Chadee, D.D. and Rawlins, S.C., 2006. Climate change impact on dengue: The Caribbean experience: University of the West Indies. *Phoenix Printery Ltd., Kingston, Jamaica*, 18, pp.5224–5238.

CPC, 2017. Cold and warm episodes by season. *http://www.cpc.ncep.noaa.gov/products/analysis_monitoring/ensostuff/ensoyears.shtml*.

CPC, 2019. ENSO: Recent evolution, current status and predictions. *https://www.cpc.ncep.noaa.gov/products/analysis_monitoring/lanina/enso_evolution-status-fcsts-web.pdf*.

Doornik, J.A., 2013. *Object-oriented matrix programming using Ox 7.0.* London: Timberlake Consultants Ltd. See http://www.doornik.com.

Duarte, J.L., Diaz-Quijano, F.A., Batista, A.C. and Giatti, L.L., 2019. Climatic variables associated with dengue incidence in a city of the Western Brazilian Amazon region. *Revista da Sociedade Brasileira de Medicina Tropical*, 52.

Durbin, J. and Koopman, S.J., 2012. *Time series analysis by state space methods.* 2nd ed. Oxford University Press.

Good, S.A., Martin, M.J. and Rayner, N.A., 2013. EN4: quality controlled ocean temperature and salinity profiles and monthly objective analyses with uncertainty estimates. *Journal of Geophysical Research: Oceans*, 118, pp.6704–6716.

Harvey, A. and Koopman, S.J., 2000. Signal extraction and the formulation of unobserved components models. *The Econometrics Journal*, 3, pp.84–107.

Huang, X., Clements, A.C., Williams, G., Devine, G., Tong, S. and Hu, W., 2015. El Niño-Southern Oscillation, local weather and occurrences of dengue virus serotypes. *Scientific reports*, 5, p.16806.

IRI, 2019. International Research Institute ENSO Forecast. *https://iri.columbia.edu/our-expertise/climate/forecasts/enso/2019-January-quick-look/?enso_tab=enso-sst_table*.

Ishii, M., Shouji, A., Sugimoto, S. and Matsumoto, T., 2005. Objective analyses of SST and marine meteorological variables for the 20th century using COADS and the Kobe Collection. *International Journal of Climatology*, 25, pp.865–879.

Kalman, R.E., 1960. A new approach to linear filtering and prediction problems. *Journal of Basic Engineering , Transactions, ASMA, Series D*, 82, pp.35–45.

Kalnay, E., Kanamitsu, M., Kistler, R., Collins, W., Deaven, D., Gandin, L., Iredell, M., Saha, S., White, G., Woollen, J., Zhu, Y., Leetmaa, A., Reynolds, R., Chelliah, M., Ebisuzaki, W., Higgins, W., Janowiak, J., Mo, K.C., Ropelewski, C., Wang, J., Jenne, R. and Joseph, D., 1996. The NCEP/NCAR 40-year reanalysis project. *Bulletin of the American Meteorological Society*, 77, pp.437–471.

Kiladis, G. and Diaz, H.F., 1989. Global climatic anomalies associated with extremes in the Southern Oscillation. *Journal of Climate*, 2, pp.1069–1090.

Koopman, S.J., Harvey, A.C., Doornik, J.A. and Shephard, N., 2010. Stamp 8.3: Structural time series analyser, modeller and predictor. *London: Timberlake Consultants.*

Koopman, S.J., Shephard, N. and Doornik, J.A., 2008. Statistical algorithms for models in state space form: SsfPack 3.0. *London: Timberlake Consultants.*

Larkin, N. and Harrison, D., 2002. ENSO warm (El Niño) and cold (La Niña) event life cycles: Ocean surface anomaly patterns, their symmetries, asymmetries, and implications. *Journal of Climate*, 15, pp.1118–1140.

Lowe, R., Bailey, T., Stephenson, D., Jupp, T., Graham, R., Barcellos, C. and Carvalho, M., 2013. The development of an early warning system for climate-sensitive disease risk with a focus on dengue epidemics in Southeast Brazil. *Stat. Med.*, 32, pp.864–883.

Lowe, R., Gasparrini, A., Van Meerbeeck, C.J., Lippi, C.A., Mahon, R., Trotman, A.R., Rollock, L., Hinds, A.Q., Ryan, S.J. and Stewart-Ibarra, A.M., 2018. Nonlinear and delayed impacts of climate on dengue risk in Barbados: A modelling study. *PLoS medicine*, 15, p.e1002613.

Lowe, R., Stewart-Ibarra, A., Petrova, D., García-Díez, M., Borbor-Cordova, M., Mejía, R., Regato, M. and Rodó, X., 2017. Climate services for health: predicting the evolution of the 2016 dengue season in Machala, Ecuador. *The Lancet Planetary Health*, 1, pp.e142–e151.

Moran-Tejeda, E., Bazo, J., Lopez-Moreno, J.I., Aguilar, E., Azorin-Molina, C., Sanchez-Lorenzo, A., Martinez, R., Nieto, J.J., Mejia, R., Martin-Hernandez, N. and Vicente-Serrano, S.M., 2016. Climate trends and variability in Ecuador (1966-2011). *International Journal of Climatology.*

Mordecai, E.A., Cohen, J.M., E., M.V., Gudapati, P., Johnson, L.R., Lippi, C.A., Miazgowicz, K., Murdock, C.C., Rohr, J.R., Ryan, S.J. et al., 2017. Detecting the impact of temperature on transmission of Zika, dengue, and chikungunya using mechanistic models. *PLoS neglected tropical diseases*, 11, p.e0005568.

NDC, 2019. Primera contribución determinada (NDC) a nivel nacional para el Acuerdo de Paris bajo la Convención Marco de Naciones Unidas sobre cambio climático. gobierno del ecuador. *Componente de Adaptación sector salud*, p.34.

Petrova, D., Ballester, J., Koopman, S.J. and Rodó, X., 2020. Multi-year prediction of ENSO enhanced by the Tropical Pacific observing system. *Journal of Climate*, 33, pp.163–174.

Petrova, D., Koopman, S., Ballester, J. and Rodo, X., 2017. Improving the long-lead predictability of El Niño using a novel forecasting scheme based on a dynamic components model. *Climate Dynamics*, 48, pp.1249–1276.

Petrova, D., Lowe, R., Stewart-Ibarra, A., Ballester, J., Koopman, S.J. and Rodó, X., 2019. Sensitivity of large dengue epidemics in Ecuador to long-lead predictions of El Niño. *Climate Services*, 15, p.100096.

Racloz, V., Ramsey, R., Tong, S. and Hu, W., 2012. Surveillance of dengue fever virus: a review of epidemiological models and early warning systems. *PLoS neglected tropical diseases*, 6, p.e1648.

Rodó, X., Rodriguez-Arias, M. and Ballester, J., 2006. The role of ENSO in fostering teleconnection patterns between the tropical north Atlantic and the western Mediterranean basin. *CLIVAR Exchanges*, 11, pp.26–27.

Ropelewski, C. and Halpert, M., 1987. Global and regional scale precipitation patterns associated with El Niño/Southern Oscillation. *Monthly Weather Review*, 115, pp.1606–1626.

Rossel, F. and Cadier, E., 2009. El Niño and prediction of anomalous monthly rainfalls in Ecuador. *Hydrological Processes*, 23, pp.3253–3260.

Santos, J.L., 2006. The impact of El Niño-Southern Oscillation events on South America. *Advances in Geosciences*, 6, pp.221–225.

Sarachik, E. and Cane, M., 2010. *The El Niño Southern Oscillation Phenomenon*. Cambridge University Press.

Sippy, R., Herrera, D., Gaus, D., Gangnon, R.E., Patz, J.A. and Osorio, J.E., 2019. Seasonal patterns of dengue fever in rural Ecuador: 2009-2016. *PLoS neglected tropical diseases*, 13, p.e0007360.

Stewart-Ibarra, A. and Lowe, R., 2013. Climate and non-climate drivers of dengue epidemics in southern coastal Ecuador. *Am. J. Trop. Med. Hyg.*, 88, pp.971–981.

Stewart-Ibarra, A.M., Kenneson, A., King, C.A., Abbott, M., Barbachano-Guerrero, A., Beltran-Ayala, E., Borbor-Cordova, M.J., Cardenas, W.B., Cueva, C., Finkelstein, J.L. et al., 2017. The high burden of dengue and chikungunya in southern coastal Ecuador: Epidemiology, clinical presentation, and phylogenetics from a prospective study in Machala in 2014 and 2015. *bioRxiv*, p.102004.

Stewart Ibarra, A.M., Muñoz, A., Ryan, S. and al et, 2018. The burden of dengue fever and chikungunya in southern coastal Ecuador: epidemiology, clinical presentation, and phylogenetics from the first two years of a prospective study. *The American journal of tropical medicine and hygiene*, 98, pp.1444–1459.

Stewart Ibarra, A.M., Muñoz, A., Ryan, S. and al et, 2019. Co-developing climate services for public health: stakeholder needs and perceptions for the prevention and control of Aedes-transmitted diseases in the Caribbean. *bioRxiv*, p.587188.

Stewart Ibarra, A.M., Ryan, S. and Beltran, E., 2013. Dengue vector dynamics (A*edes aegypti*) influenced by climate and social factors in Ecuador: Implications for targeted control. *PLOS ONE*, 8, p.11.

Trotman, A., Mahon, R., Shumake-Guillemot, J., Lowe, R. and Stewart-Ibarra, A.M., 2018. Strengthening climate services for the health sector in the Caribbean. *Bulletin of the World Meteorological Organization*, 67(2).

Vincenti-Gonzalez, M., Tami, A., Lizarazo, E. and Grillet, M., 2018. Enso-driven climate variability promotes periodic major outbreaks of dengue in Venezuela. *Scientific reports*, 8, p.5727.

Xiao, J., Liu, T., Lin, H., Zhu, G., Zeng, W., Li, X., Zhang, B., Song, T., Deng, A., Zhang, M. et al., 2018. Weather variables and the El Niño Southern Oscillation may drive the epidemics of dengue in Guangdong Province, China. *Science of the total environment*, 624, pp.926–934.

Zhang, Q., Chen, Y.F., Liu, T., Zhang, Q., Guo, P. and Ma, W., 2019. Epidemiology of dengue and the effect of seasonal climate variation on its dynamics: a spatio-temporal descriptive analysis in the Chao-Shan area on China's southeastern coast. *BMJ open*, 9, p.e024197.

Acknowledgements:

JB gratefully acknowledges funding from the European Union's Horizon 2020 research and innovation programme under grant agreements No 727852 (project Blue-Action), 730004 (project PUCS) and 737480 (Marie Sklodowska-Curie fellowship ACCLIM).

RL was supported by a Royal Society Dorothy Hodgkin Fellowship.

AMSI was supported by NSF DEB EEID 1518681.

Author contributions D.P. designed the study, carried out the ENSO and local climate forecasting, analysed the data and wrote the manuscript. R.L. designed the study, provided the dengue forecasts and contributed to the writing of the manuscript. R.S. prepared the dengue and local climate data into monthly time series, R.M. provided the weather station data, A.S.I, M.B.C., G.M.V and A.A.O provided the dengue data. All authors contributed to the discussion and presentation of results and to the revision of the manuscript. The authors declare no competing financial interests.

List of Figures

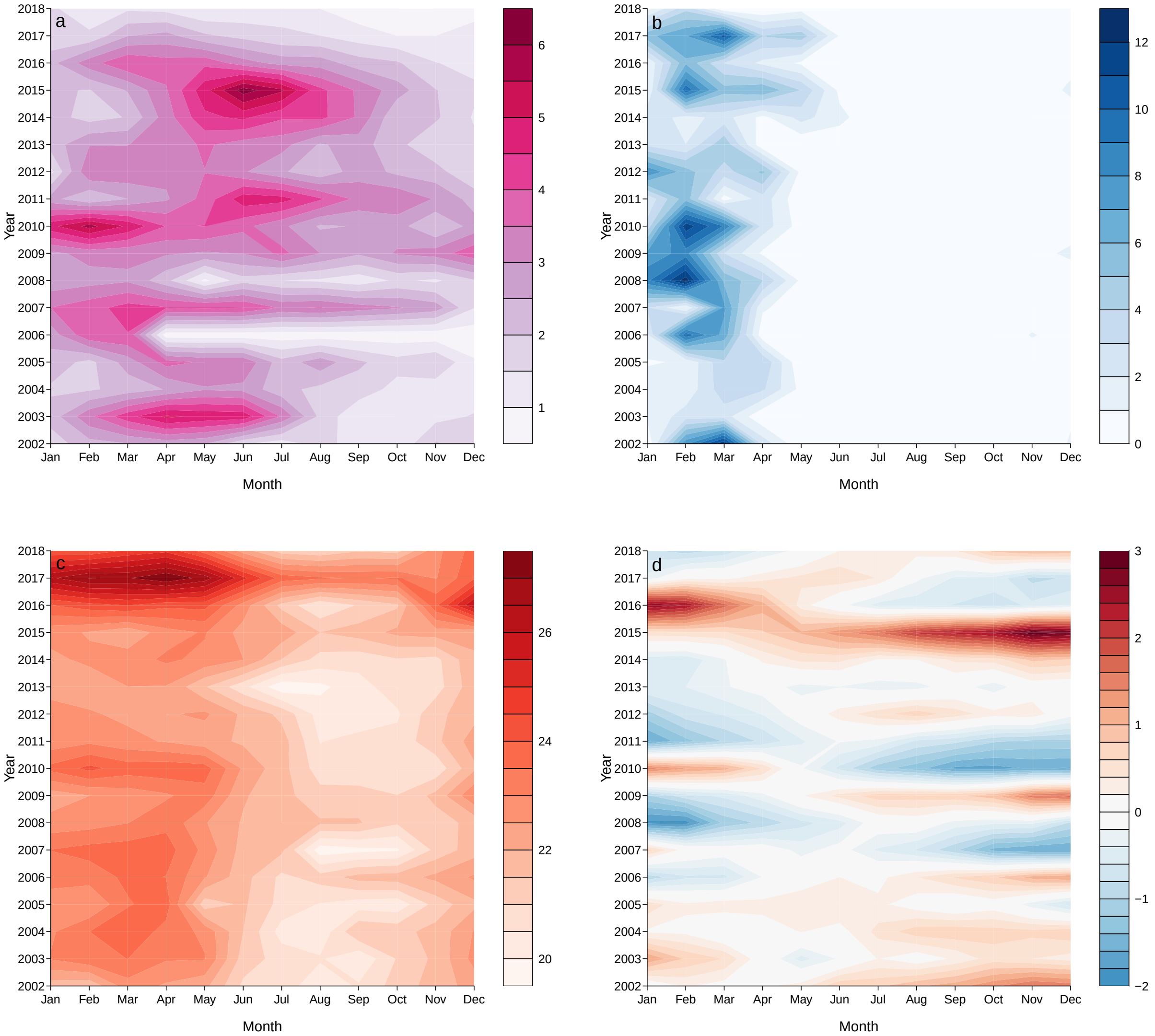

Figure 1: (a) Dengue incidence in Machala, Ecuador (cases per 100,000 inhabitants) (b) precipitation (mm/month) and (c) minimum temperature (°C), from the Granja Santa Ines weather station (2002-2016) and Hospital Teófilo Dávila weather station (2017-2018), located in Machala and (d) Niño 3.4 index (sea surface temperatures (SST) anomalies (°C) in the Niño 3.4 region) at the monthly time scale from January 2002 to December 2018.

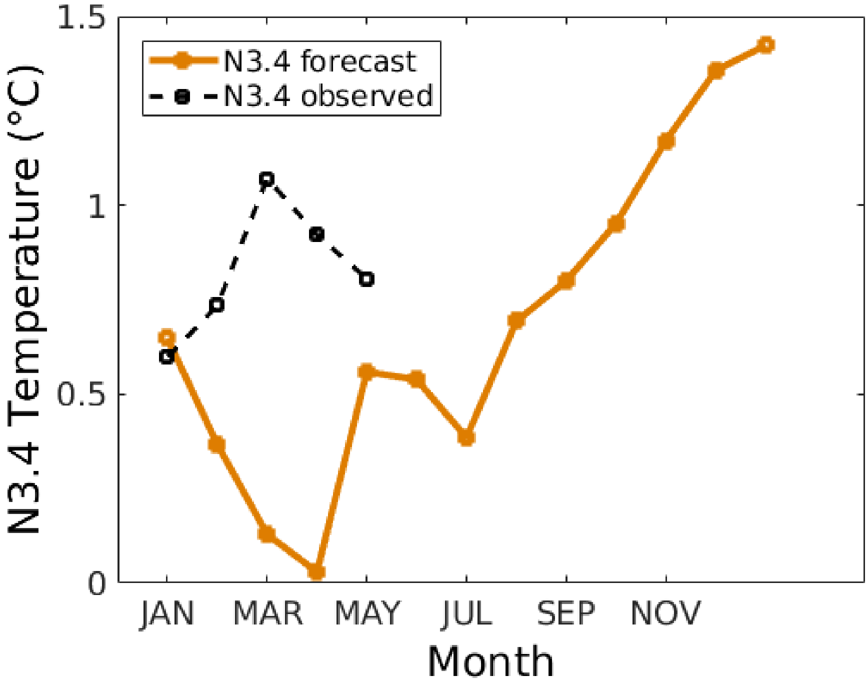

Figure 2: Forecast of the sea surface temperature anomaly (°C) in the Niño3.4 region from January to December 2019 at progressively increasing lead time from 1 to 12 months (beige curve), and observation values from January to May 2019 from NOAA-OI-SST-V2. The anomalies are calculated by subtracting the mean annual cycle over the period 1982-2012.

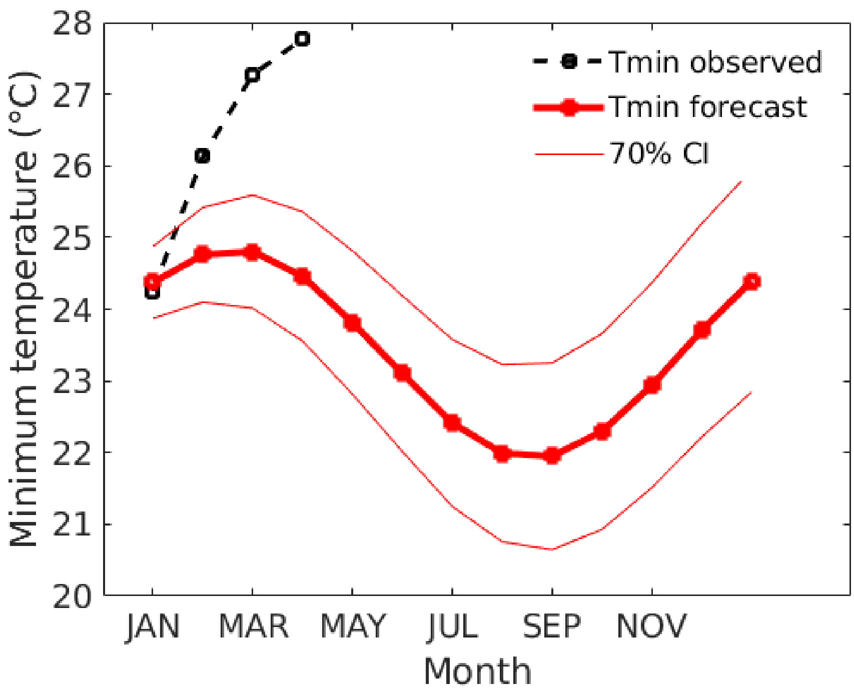

Figure 3: Monthly forecasts of minimum temperature (°C) for Machala, Ecuador, from January to December 2019 (thick red curve), 70% CIs (thin red curves), and observations from the Hospital Teófilo Dávila weather station located in Machala for January to April 2019.

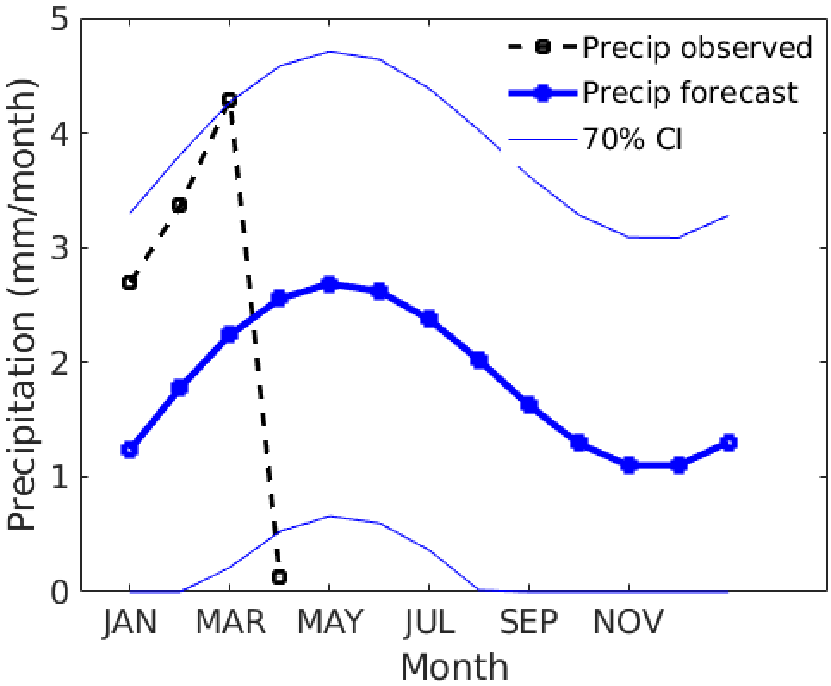

Figure 4: Monthly forecasts of precipitation (mm/month) for Machala, Ecuador, from January to December 2019 (thick blue curve), 70% CIs (thin blue curves), and observations from the Hospital Teófilo Dávila weather station located in Machala for January to April 2019.

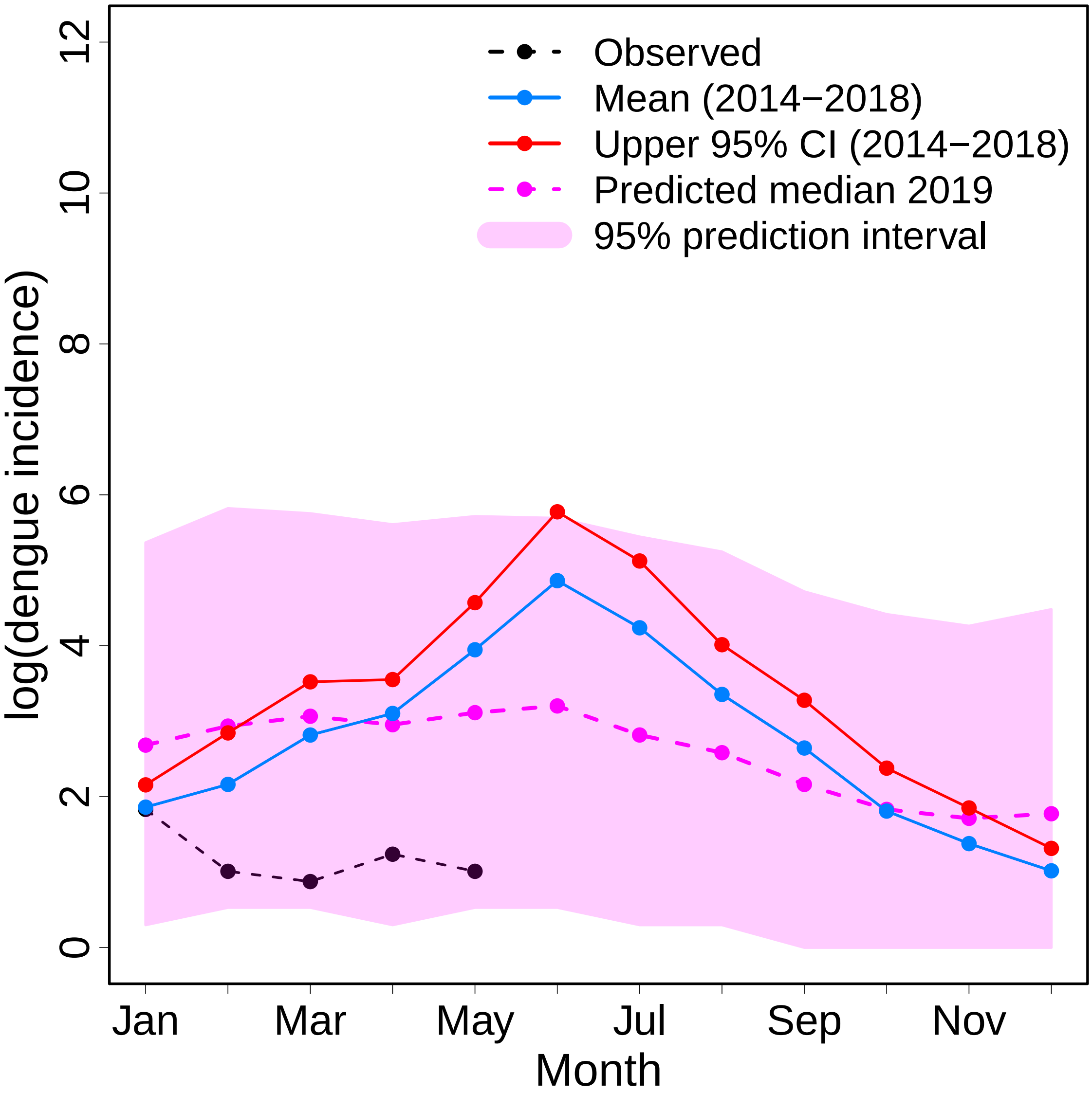

Figure 5: Posterior predicted median (dashed purple curve) and 95% prediction (credible) interval (purple shaded area) for log dengue incidence rates (cases per 100,000 population) in Machala, Ecuador, January - December 2019. The five-year mean dengue incidence (blue curve) and upper 95% confidence interval (red curve), for the period 2014-2018, is shown. Observed dengue incidence rates are also included (dashed black curve).

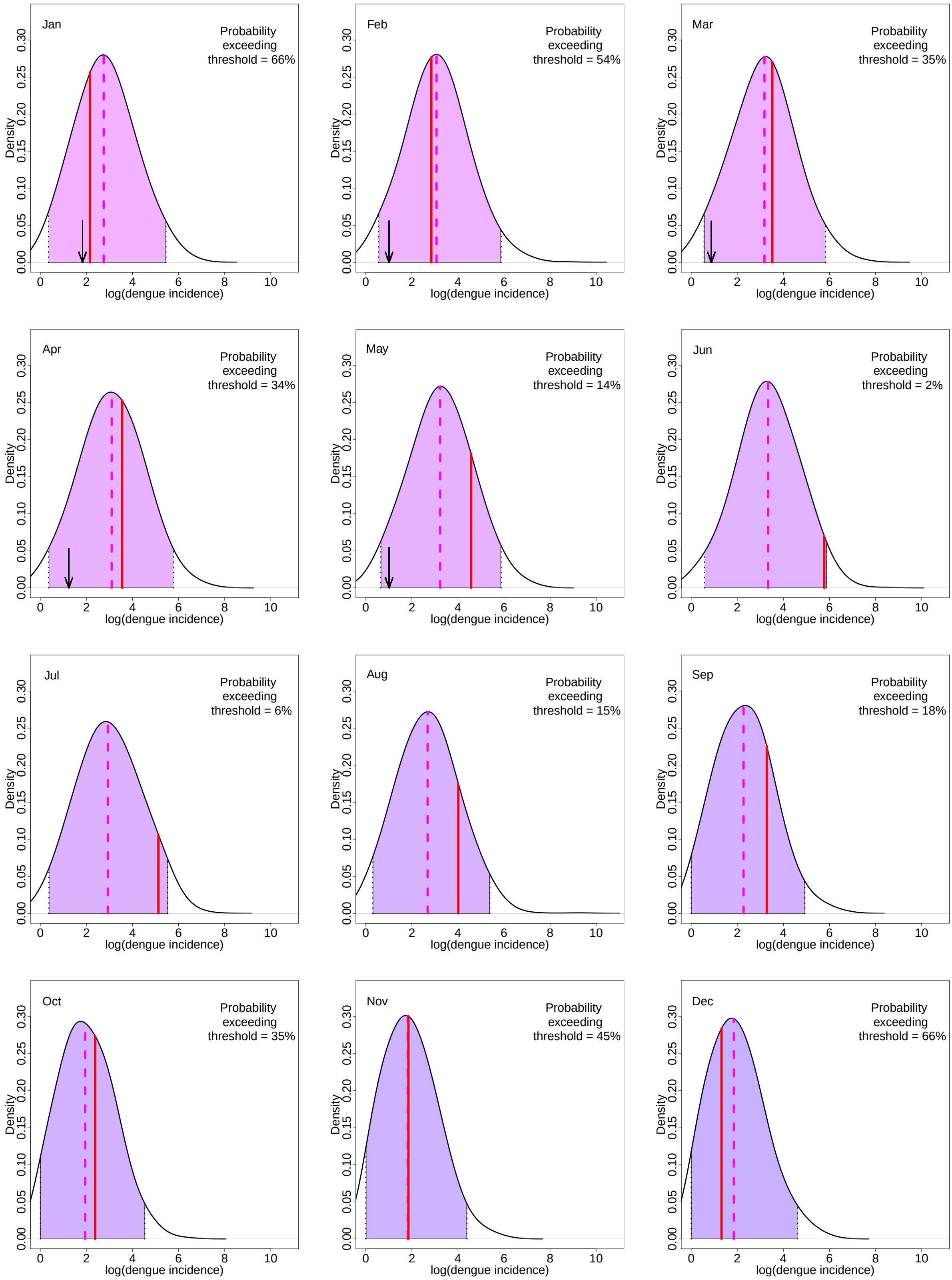

Figure 6: Posterior predictive distribution of dengue cases (logarithmic scale) for January - December 2019, showing the probability of exceeding the upper 95% confidence interval (red solid line). The posterior predicted mean (dashed line), 95% credible intervals (dotted lines) and observed dengue cases (where available, arrow) are indicated.